Detection of the Tip of the Red Giant Branch in NGC 3379 (M105) in the Leo I Group (DRAFT 3/11/96)

Shoko Sakai

Jet Propulsion Laboratory, California Institute of Technology

MS 100-22, Pasadena, CA 91125

shoko@ipac.caltech.edu

Barry F. Madore

NASA/IPAC Extragalactic Database, Infrared Processing and Analysis Center

California Institute of Technology, MS 100 22, Pasadena, CA 91125

barry@ipac.caltech.edu

Wendy L. Freedman

The Observatories, Carnegie institution of Washington

813 Santa Barbara Street, Pasadena, CA 91101

wendy@ociw.edu

Tod R. Lauer and **Edward A. Ajhar**

National Optical Astronomy Observatories

P.O. Box 26732 Tucson, AZ 85726

lauer,ajhar@noao.edu

and

William A. **Baum**

Department of Astronomy, FM-20

University of Washington, Seattle, WA 98195

baum@astro.washington.edu

Running Headline: *TRGB Distance* to *NGC* 3379

Received —. —.- . . . . .-------- accepted _____

ABSTRACT

We report the unambiguous detection of individually resolved stars in the elliptical galaxy NGC 3379, a luminous member of the Leo I Group. The bright end of the stellar luminosity function has a logarithmic slope that is consistent with these stars being Population II red giants. An abrupt discontinuity in the apparent luminosity function at $I = 26.29 \pm 0.09$ mag is identified with the tip of the first- ascent red giant branch (TRGB). Adopting $M_I(\mathrm{TRGB}) = -4.0 \pm 0.1$ mag gives a distance modulus of 30.29 ± 0.28 mag corresponding to a linear distance to NGC 3379 of 11.4 ± 1.3 Mpc. The TRGB distance compares very well with the Cepheid distance of 11.6 ± 0.8 Mpc (30.32 ± 0.16 mag) to another group member M96 (= NGC 3368). The distance to NGC 3379 can be used in turn to calibrate the zero points of four other distance indicators: surface brightness fluctuations, planetary nebula luminosity functions, globular cluster luminosity functions and the $D_n - \sigma$ method. We apply two approaches to measuring the Hubble constant: (1) a simple Virgocentric infall model, and (2) stepping out from Leo I to the Coma cluster using the previously measured relative distance between the two clusters. Both techniques give a value of Hubble constant consistent with $H_0 = 68 \pm 13$ km s^{-1} Mpc^{-1}.

Subject headings: galaxies: individual - galaxies: elliptical galaxies – galaxies: distances

1. Introduction

There are several paths to a far--field estimation of the Hubble constant. However these paths are often complicated by a series of arguable, but necessary, assumptions, where external checks and comparisons can be difficult, or impossible due to largely non-overlapping data sets. On the other hand, various measures of the near-field distance scale (largely made within the Local Group) are in excellent agreement, having benefited from numerous recent intercomparisons of distances to the nearest galaxies. Using both Population I and Population 11 distance-determination methods the local distance scale appears to have converged at the ±10 – 20% level (see Freedman & Madore 1993, 1995; Hutterer, Sasselov & Schechter 1995). Cepheids have long been the cornerstone of the Population 1 route; and RR Lyraes have more recently provided the best Population 11 counterpoint. But RR Lyme stars are intrinsically fainter than classical Cepheids, making their application to galaxies significantly beyond the Local Group unlikely in the foreseeable future.

There are, however, Population 11 stars brighter than the horizontal branch variables. Indeed, the brightest red giant branch (RGB) stars, identified by their first appearance as a discontinuity in the bright end of the luminosity function of the first-ascent (Population 11) RGB population has also been shown to be extremely stable in luminosity, while being some 40 times brighter than the RR Lyrae stars. In the I–band, this TRGB ("tip-of-tile-red-giant-branch") method as a distance indicator is only slightly sensitive to metallicity over a wide range of ages and metallicities applicable to old galaxy populations (see Lee, Freedman & Madore 1993).

The tip of the first- ascent red giant branch marks the core helium flash of low-mass stars which evolved along the red giant branch up to the tip, at which point the luminosity function abruptly terminates. In *I* - band, the TRGB resolves at $M_I \sim$ - 4 mag. This

discontinuity has been shown to be an excellent distance indicator, since the bolometric luminosity of the TRGB varies only by NO.] mag for ages ranging from 2 up to 15 Gyr (cf. Iben & Renzini 1983), and metallicities in the range represented by Galactic globular clusters (–2,1 $\leq$[Fe/II]$\leq$ --0,7). Theoretically predicted and now empirically tested and confirmed, the TRGB is an outstanding distance indicator. Furthermore, it is applicable to all morphological types of galaxies. Since they represent the evolved component of older generations of stars in galaxies, TRGB stars are naturally found in elliptical galaxies, spiral disks and halos, as well as in irregular galaxies.

An agreement between the distances derived from the Cepheid PL relation and TRGB method is remarkable. Distances to about a dozen galaxies have now been measured by two methods and they agree with each other within 0.1 mag (Lee, Freedman & Ma(lore 1993, Sakai, Madore & Freedman 1996). It is important to note the significance of the TRGB method as a pure application of a Population II distance indicator. Several secondary - distance indicators which enable us to investigate the density and velocity fields at cosmologically - significant distances, including surface brightness fluctuations, planetary nebula luminosity functions, globular cluster luminosity functions, and the D_n -- σ relation, all strongly depend on the old E/S0 galaxy populations. Since Cepheid variables are not found in these systems, and because of the lack of elliptical systems within or even near to the Local Group, the absolute calibration of such Pop 11 methods has either had to rely on the distance to a single galaxy (*e.g.* the bulge of M31), or Cepheid (Pop 1) distances to spiral galaxies in the same group or cluster. The TRGB method could be used as an alternative calibrator. Since this method is calibrated by RR Lyrae distances to Galactic, globular clusters, it dots not provide a direct distance to tile target galaxy. In this sense, the TRGB method is very similar to the surface brightness flue.tuatiou method. However, it is significant that we arc indeed directly measuring the magnitudes of individual stars. In that sense, the TRGB method resembles the Cepheid method, and has a potential as a

Population 1 I calibrator.

Using computer simulations, Madore & Freedman (1995) have investigated the distance out to which the TRGB method is applicable They conclude that from the ground under optimal conditions of seeing, the method could be used for galaxies out to at least 3 Mpc and that distances up to $\sim$ 13 Mpc can be achieved with the *HST*. Distances slightly in excess of 1 Mpc have already been measured from the ground using the TRGB under moderate (1.3 arcsec) seeing conditions (e.g., Sakai, Madore & Freedman 1996). We report here the first space based application of this method to an elliptical galaxy, NGC 3379 in the Leo I Group. This constitutes the most distant application of the TRGB method to date, and its first application to a giant elliptical galaxy.

Using data obtained with the *Hubble Space Telescope* (*HST*), wc present in the next section observation.s and data reduction procedures, followed by the application of the TRGB method to the I-band luminosity function for stars in the halo of NGC 3379. We conclude by presenting some implications for the value of Hubble constant.

2. Observations and Data Reduction

A primary goal of the *HST* observations was to study the I-band RGB luminosity function down to depths close to the Tonry & Schneider (1988) I-band fluctuation magnitude, $\bar{M}_I = -1.5$, which for a distance to NGC 3379 of 10.6 Mpc, corresponds to $\bar{m}_I \approx 28.6$. Resolving such stars required the target field to be in the extreme outer envelope of NGC 3379. De Vaucouleurs & Capaccioli (1979) presented a B-band photometric trace of NGC 3379 running along the cast-west vector cutting through the center of the galaxy. The trace goes out to extremely large angular distant.cs from the center of NGC 3379, and thus to extremely faint surface brightness levels (see also Capaccioli *et al.* 1990). Wc selected the pointing to be 6 arcminutes west, of the nucleus at $\alpha_{2000} = 10^h\ 47'''\ 49\overset{s}{.}4$ and

$\delta_{2000} = 12°\ 34'\ 57\farcs1$, which is an empty field on the POSS-I print of the area (Figure 1). A deep I-band CCD image of the field (Figure 2), however, confirms the photometry of de Vaucouleurs & Capaccioli (1979) in a qualitative sense by showing the envelope of the galaxy to extend at least out to this area. At this location, de Vaucouleurs & Capaccioli (1 979) find the galaxy surface brightness to be $\mu_B \approx$ 27,1, which corresponds to typical galaxy brightness of $m_I \approx$ 30.9, per WFC pixel, assuming $V - I = 1.2$. At this surface brightness there are $\sim$1 2 "fluctuation stars" per square arcsec, thus giving excellent resolution for exploring the brighter tip of the luminosity function. In passing, we note that we selected a west rather than east field as de Vaucouleurs & Capaccioli (1979) showed that NGC 3384 overlaps significantly with NGC 3379 at large distances east of the NGC 3379 center.

The observations of NGC 3379 were made in May 1994, using the Wide Field/Planetary Camera-2 (WFPC2). Thirty-two 900s exposures were taken in the 1"814W filter, yielding a total exposure time of 8 hours. An attempt was made to dither the pointing in a 2 x 2 grid of 0,5 WFC pixel spacings to obtain Letter spatial resolution, thus the full exposure sequence consists of 4 sets of 8 exposures taken in sequence. Unfortunately, this was one of the earliest attempts at dithering and after each set of 8 exposures, the *HST* guiding was reset, resulting in pointing differences of a few pixels rather than the precise half-steps desired. As it happened, however, the fractional portion of the pixel shifts did fall close to three of the four desired substeps, thus the full set still contains significantly more information than 32 identical pointings would, even if the sampling is not as desired. A portion of the WF4 field, for which an attempt at building the substepped image has been made, is shown in Figure 3. The envelope of NGC 3379 has clearly been resolved into its red giant stars.

The data quality files, provided by the HST data- processing pipeline, and vignetting

masks were used to mark bad pixels on the images. '1'0 deal with the problem of the geometric distortion of the WFPC2 optics, wc used the pixel area map provided by Holtzman to restore the integrity of tile flux measurements. once the galaxy images were processed through these steps, all 32 frames were combined using an IRAF routine "imcombine" with the 3-σ clipping option to remove obvious cosmic rays.

The stellar photometry was then carried out using the packages DAOPHOT and AI, LSTAR (Stetson 1987). These programs usc automatic star finding algorithms and then measure stellar magnitudes by fitting a point-spread function (PSF), constructed from other uncrowded images (Stetson 1994). We tested for a possible variation in the luminosity function as a function of the position on each chip by examining the luminosity functions for inner and outer half of the frames. For each chip, wc obtain essentially the same luminosity function, confirming that there is no systematic offsets in measured PSF magnitudes. The F814W-filter PSF magnitudes were transformed to Cousins I and corrected to l-see exposure time, following the calibration prescriptions given by Holtzman *et al.* (1995). The transformation equation is:

$$I = m_{DAOPHOT} + 2.5 \log t - C, \quad (1)$$

where C equals 1.916 mag for WF2, 1.913 for WF3, and 1.942 mag for WF4. Since wc only have I-band observations of N3379, no color information on the stars is available. 1 lowever, the color term in the calibration is small, expressed as:

$$0.063(V - I) - 0.025(V - I)^2 \quad (2)$$

Then the color correction would amount to approximately 0.04 mag at most (2% in distance) even for $(V - I)$ of 2, the color of a very red giant branch. We note that the integrated color of the central portion of this galaxy is $(V - I) = 1.2$ mag (Tonry *et al.* 1 990). However, our data presented in this paper is 6 arcmin away from tile nucleus. Thus, the color in this part of the halo is unknown.

3. The Luminosity Function

Using DAOPHOT, we have found ~13,000 objects on each chip. In order to discriminate non-stellar objects, such as background galaxies, we use the χ^2 value which is one of the standard fitting parameters reported by ALLSTAR, giving the goodness of fit of PSF to the object profile itself. Limiting the database to objects with χ^2 <1.6 (effectively selecting the most likely stellar candidates), we reduced the number of objects down to ~1 500 per chip. This is rather a conservative selection of objects. We have also checked the brightest stars ($I \leq$ 27.0 mag) visually on each chip to make sure that they were not contaminated by background galaxies.

Although no color information is available, the form and slope of the observed I-- band luminosity function for star-like objects in the NGC 3379 frames, as shown in Figure 3, present compelling evidence that what we are seeing is indeed the first--ascent red giant branch. The abrupt, turn-on of the luminosity function is *prima facia* evidence that we have resolved Population II stars. Top panels in Figur e 3 shows the I--band luminosity function for the stellar data found on all chips. We have only included those stars with photometric errors less than 0.20 mag in this analysis. The rapid rise in the numbers of stars at $I \sim 26$ mag shows unmistakably the TRGB. Following this, there is a shallower but still monotonic rise in the counts up to $I \sim$ 27.2 mag at which point incompleteness due to photon statistics takes over and truncates the data (see bottom panel in Figure 3).

The numbers of stars at a particular location in an observed color-magnitude diagram is simply proportional to the amount of time stars spends in that stage of evolution. Thus, the observed ratio of numbers of extended, intermediate-age asymptotic giant branch (AGB) stars to first red giant branch (RGB) stars can be compared with the predicted ratio of lifeti mes in the two phases so as to place quantitative limits on the fraction of 4-5 Gyr AGB stars in nearby resolved galaxies (*e.g.*, Mould, Kristian and Da Costa 1983; Freedman

1989).

Stars of ages 4-5 Gyr will extend approximately 1 bolometric magnitude above the TRGB (e.g., Mould and Da Costa 1988). The estimated lifetime for stars in this phase *is* about 10^6 years (Iben 1988). In the one-magnitude interval just below the TRGB, the lifetimes arc estimated to lie in the range of 3-5 x 10^6 years (Sweigart and Gross 19'78), Hence, for an inter-mediate age population the predicted ratio of extended AGB to RGB stars ranges from 0.2-0.3.

There are 76 and 1867 stars located one magnitude above and below the TRGB, respectively. Allowing for the presence of a '20% component of fainter AGB stars in the magnitude bin below the TRGB (Lee 1977; Mould, Kristian & Da Costa 1983) results in a derived ratio of 0.05. This is a factor of 4-6 times smaller than that predicted above for a population of 4-5 Gyr AGB stars. Hence, the fraction of stars which can belong to a younger AGB population is limited to about 20%.

4. The TRGB Distance

From previous work (see Lee, Freedman & Madore 1993; Madore & Freedman 1995 and references therein), we expect to detect stars achieving the peak luminosity along the first- ascent red giant branch at an absolute I-band magnitude of -4.0 mag. It has been demonstrated empirically, and there is a theoretical basis for expecting that in the specific wavelength range defined by the I--band filter ($\sim$8000 Å), the absolute magnitude of the TRGB is quite insensitive to age and metallicity. Residual metallicity effects on the absolute magnitude nave been calibrated over the metallicity range of Galactic globular c.lusters (Lee, Freedman & Madore 1993), making the I-band magnitude of the TRGB a stable and luminous Population II extra.galactic. distance indicator. Outside the calibration range, however, the higher metallicity may affect the Ills.gylitudc of the TRGB considerablly.

Dur to line--blanketing effects, the TRGB magnitude is known to become fainter at higher metallicities. The photometric studies of the high-metallicity Galactic globular clusters seem to indicate such behavior in the $(V - I)$ color magnitude diagrams. '1'here has been no solid calibration of the TRGB magnitude for metallicities $[Fe/H] \geq$ --0.7. We will discuss the impact of this issue in particular with respect to NGC 3379 in later sections.

We use both a kernel- smoothed linear luminosity distribution and the logarithmic luminosity function to determine the luminosity of tile TRGB. When the adopted edge detection filter is applied to a distribution having a sudden discontinuity on the bright side leading to a constant-slope distribution on the faint side (such as the one sought here), the filter output will show a significant positive response at the discontinuity followed by a plateau at the new slope (see Figure 1 in Madore & Freedman 1995). In Sakai, Madore & Freedman (1996), wc introduced a kernel-smoothed luminosity function (but not logarithmic) filtered by a modified Sobel kernel; here, wc apply the identical edge detection filter to the logarithmic luminosity distribution as well to determine the magnitude of the TRGB. The logarithmic luminosity function is preferred because of its characteristic slope of 0.6 mag/dex for the RGB population which should be more easily detected by the edge-detectioll filter. In addition, we apply a weighting scheme to the filtered response function. The edge detection filter essentially measures the slope, and thus it is extremely sensitive to noise; any sudden change in signal is amplified by the filtering scheme. If the luminosity function is expressed by $\Phi(I)$, the response function at I is derived via $E(I) =$ log $\Phi(I+\sigma)$ - log $\Phi(I-\sigma)$ where σ is a typical error for stars of magnitude I (see Appendix of Sakai, Madorc & Freedman 1996 for details), Each $E(I)$ is weighted by a square root of $\Phi(I)$. The weighting scheme was used in order to suppress those responses that are statistically nonsignificant due to noisy data. In Figure 4, the smoothed I- -band luminosity functions and the corresponding response functions from the edge detection filtering are plotted. Inspecting both response functions, we report an

unambiguous detection of the TRGB at I : 26.314-0.05 msg. The WF4 field is least contaminated by background galaxies and its stellar population is the dominant source of signal in the combined response function.

However, note also that there is a substantial signal at I = 25.9 mag in the logarithmic representation of the data, Could this be the TRGB? This appears unlikely because, as shown below, this peak is not a robust feature. We studied the reliability of each signal by calculating the error in each bin in the response function histogram. If the ith magnitude bin has N_i counts, its Poisson error is simply $\sqrt{N_i}$. For each luminosity function bin, we perturbed its number randomly following a Gaussian distribution whose dispersion was set to $\sqrt{N_i}$. For each iteration of randomly displaced luminosity function, wc re- applied the edge- detection filter and measured the response function. An average response histogram of all 500 iterations is plotted in Figure 5. The 1 σ errors for each bin arc also shown. It is clear that all the 'signals' below I =. 26.0 mag are very likely due to noise, while the TRGB signal remains stable.

Taking into account the Galactic extinction correction along the line of sight to NGC 3379, which amounts to only 0.02 mag (Burstein & Heiles 1978) in the I-band, we adopt I_o = : 26.29 mag for the TRGB. It is assumed that the internal reddening in NGC 3379 is negligible as the target field is placed 6 arcmin away from the nucleus, and we apply no correction here. The TRGB distance modulus is derived via a relation $(m - M)_{TRGB} = I_{TRGB} + BC_I$ -- $M_{bol,TRGB}$ where BC_I is the bolometric correction to the I magnitude and $M_{bol,TRGB}$ is the bolometric magnitude of the TRGB stars (Lee *et al.* 1993). BC_I and $M_{bol,TRGB}$ are expressed in terms of metallicity and color: BC_I = 0.881 -- $0.243(V - I)_{TRGB}$ and $M_{bol,TRGB}$ = - $0.19[Fe/H]$ --3.81. We must then address what the metallicity of the TRGB halo stars is for NGC 3379. The integrated color of this galaxy is reported to be $(V - I)$ = *1.2* (Tonry *et al.* 1990); but unfortunately,

no published ground--based surface photometry reaches deep enough to determine the color at the position of the WFPC2 field, 6 arcmin from the nucleus. However, there are several studies which indicate that the halo of NGC 3379 is blue enough to apply the TRGB calibration of Galactic globular clusters, Sodeman & Thomsen (1994) presented a deep]--band profile of this galaxy to large radius. They reported a color gradient in $(B - I)$ out to 100" where it fell to $(B -- I) = 1$ .97+ 0,10 mag from the central value of $(B - I) =$ 2,14 msg. They obtained the gradient of $\Delta(B - I)/\Delta \log r =$ -0.153:0.02 mag, suggesting that the color of the NGC 3379 halo is already getting reasonably blue at $r =$ 100". Davies, Sadler & Peletier (1 993) measured Fe and Mg line--strength gradients for 13 elliptical galaxies out to effective radius, and showed that the envelope becomes metal poorer as a function of the radius. The work by Davidge & Clark (1994) also suggested a tendency for metallic absorption features to weaken with increasing radius. Both of these studies support an elliptical galaxy halo that is metal poorer, and that the color gradient may indeed be indicative of the metallicity gradient. Using the photometry results of Sodeman & Thomsen, at $r =$ 360" where the WFPC2 observations were made, the color reaches $(B - I) =$ 1.89 :I 0.15 mag. Substituting this value into a relation $[Fe/H] = 2.67(B - I)$ --- 5.73 derived from Couture *et al.* (1990), we obtain $[Fe/H] =$ -0.6840.16 dex. This is only marginally outside the solid calibration of the TRGB. The original calibration of the TRGB method by Lee *et* al. (1 993) applies strictly only to the metallicity range of --2.2< $[Fe/H]$ <- 0.7.

Given the understanding that the metallicity of NGC 3379 halo is slightly outside the! Galactic globular cluster metallicity calibration range, we proceed to determine the absolute magnitude of the TRGB for NGC 3379 following Lee *et al.* (1993), and carry the uncertainty in the metallicity calibration in our total error budget, discussed in Section 8 below. We obtain $M_I =$ -4.03 0.14 mag. Thus, the TRGB distance modulus for NGC 3379 is 30.294 0.28 mag. This corresponds to a linear distance of 11.4 :I 1.3 Mpc.

There are, however, potential systematic errors that need to be accounted for as well, The uncertainties in the measured TRGB distance will be discussed in details in Section 8.

5. Comparison with Previously–Published Distances

Within the last 6 years, three new and relatively independent determinations of the distance to NGC 3379 have been published. Ciardullo *et al. (1989)* have used the planetary nebula luminosity function method to estimate a distance of 10.0 Mpc ($\mu_o = 30.01$ mag). Tonry (1993) have estimated the distance to NGC 3379 using the surface brightness fluctuation (SBF) method, and they derive 9.4 Mpc ($\mu_o = 29.87$ mag). Finally, Pahre and Mould (1 995) have also used the SBF method, but applying it in the near infrared K-band rather than in the optical; they obtain a distance of 11.1 Mpc ($\mu_o = 30.22$ mag). All of these previous determinations rely on a zero point calibration based on the Cepheid determination to M31, (and, in some cases, the companions to M31). Our TRGB distance agree with the Sill' and PNLF results within 3σ, which is encouraging. In section 8 in which we discuss the error budget, wc will show that systematic errors would put the distance presented here as the upper limit.

6. The Leo I Group

The Leo 1 Group (= M96 Group =-- G 1'2 according to dc Vaucouleurs 1975), consists of five dominant galaxies: NGC 3368 [M96; SAB(rs)ab], NGC 3351 [M95; SB(r)b], NGC 3384 [S11(S)0], NGC 3377 [E5/6] and NGC 3379 itself [M105; it]]. Two of its spiral members NGC 3368 and NGC 3351 have been the focus of initiatives to measure their distances using Cepheids discovered by *HST* (Tanvir *et al.* 1995; Graham *et* al. 1996) respectively. At this time, only the data for NGC 3368 (: M96) have been published and they give a

true distance modulus of 30.3240.16 mag which corresponds to a linear distance of 11.6 + 0.8 Mpc. The close agreement of the Cepheid distance to NGC 3368 and the TRGB distance to NGC 3379 is encouraging, and provides some support for the compact nature of the M96/Leo Group and the physical association of the spiral galaxy NGC 3368 with the dominant ellipticals in the group,

7. The Hubble Constant

A search of the NED database reveals 15 galaxies, within a radius of 5 degrees of M96 and having published radial velocities less than 1,200 km s-l. Their mean velocity in the reference frame of the Local Group (corrected using $V_{LG} = V_{Hel}$ + 300 sin 1 cos b) is + 715 km S''. Within the group, those 15 galaxies have a. velocity dispersion of ±178 km s^{-1}, giving an uncertainty on the mean redshift of ± 46 km s^{-1}.

In the following sections, we estimate the Hubble constant via two separate routes. First, wc give a simple estimate of H_0 correcting the Leo I velocity field for Virgocentric infall. Wc then proceed to estimate H_0 based on a calibration of secondary methods based on our TRGB distance to NGC 3379.

7.1. Virgocentric Infall Model

We now proceed to evaluate the local expansion rate using the most direct (although still overly simplified) approach in which the smooth, unperturbed expansion velocity of NGC 3379 is determined by considering a single perturbation flow model involving only the Virgo cluster. Using simple geometry (Figure 4), the Virgocentric infall of the Leo I group can be estimated by scaling the amplitude of the Local Group infall velocity into the Virgo cluster. For instance, Mould *et al.* (1 995) quote 33] ±41 km S-1 for the Local

Group infall velocity toward Virgo, We adopt that value here and take the distance to the Virgo cluster from the Local Group to be 16.1 ± 3.2 Mpc (Ferrarese *et al.* 1996); the large uncertainty here is adopted to reflect the complex geometry of the Virgo cluster. By simple trigonometry, and using linear perturbation theory with an assumption that the density profile of the Virgo cluster varies as r-z, wc find that the infall velocity of Leo 1 Group towards Virgo is 7073:88 $km\,s^{-1}$. A rough sketch of the velocity field is shown in the right pane] of Figure 6. The radial component of Leo's infall along the line of sight from the Local Group to Leo 1 is then +326 ± 37 km s^{-1}. In addition to this, there is of necessity a component of the Local Group infall into Virgo projected along the line of sight to Leo. This component is -301 ± 37 km S-l. We note in passing that these two terms are almost equal in magnitude but opposite in sign, therefore largely canceling each other in the fins] determination of the pure expansion velocity of Leo. Removing the infall components from the observed recession velocity, the unperturbed expansion velocity of the Leo I Group in this mode] is then + 715 – 315 -1 301 = +704 ± 70 km s^{-1}. The Hubble constant derived directly from the velocity field at the 11.4 Mpc distance of the Leo I Group is 62 ± 6 km $s^{-1}Mpc^{-1}$. A full non-linear perturbation analysis including the correlated nature of the errors suggests a more robust solution with a mean value and error of 67 ± 14 km s^{-1}.

The foregoing calculations all assume that there arc no additional perturbations to the Local flow model outside of the Virgo infall, and that there arc 110 transverse peculiar motions of either the Leo or the Local Group, Moving to larger redshift-distances would alleviate the effects of additional random motions which are not easily measured independently. We can now proceed to estimate the Hubble constant using the secondary distance indicators.

7.2. Calibration of Secondary Distance Indicators

In this section, we explore how our TRGB distance to NGC 3379 can be applied to calibrate some of the Population II secondary distance indicators. We are not by any means providing the new calibrations for these methods; rather our purpose here is to demonstrate as an exercise how the problem of the lack of solid calibrators in the Population 11 methods could be solved,

Surface **Brightness Fluctuations:** This method is primarily applied to giant elliptical galaxies. It basically measures the second moment of the luminosity function, which is a calibrated function of the $(V - I)$ color (Tonry 1991, Jacoby *et* al. 1992). " Application of the SBF method to nearby clusters shows that it has a small intrinsic dispersion of $\pm$ 0.08 to $\pm$0.15 mag in the I- band (Tonry 1991). However, only one local calibrator distance was available to Tonry (1991), the M31 bulge. Recent discovery of Cepheid variables in M81 (Freedman *et al.* 1994), has supplemented the sample of calibrators, but again, it is the bulge of M81 that is applied in the SBF calibration, It is uncertain at present whether a systematic difference exists between these calibrators and the target galaxies which arc mostly giant elliptical galaxies. Here, wc attempt to calibrate the SBF method using our TRGB distance to NGC 3379 and show how it can be used to resolve this problem.

The mean fluctuation magnitude is expressed by

$$\bar{M}_I = C + 3(V - I)_{\rm obs} \qquad (3)$$

where C is the zero point, for which Tonry (1991) derives C = 4.84 mag. The distance modulus is then written as:

$$(?,2 - M)_{\rm SBF} = \bar{I}_{\rm obs} - C - 3(V - I)_{\rm obs} + 0.80 A_B, \qquad (4)$$

where A_B is the extinction in B- band.

We rederive the zero point of the SBF method using the TRGB distance to NGC 3379.

We assume that the distance to M31 is 770 kpc which corresponds to the distance modulus of 24,43 mag (Freedman & Madore 1990). All the necessary data were taken from Table 2 in Ciardullo, Jacoby & Tonry (1993: CJT). The zero point determined by using only NGC 3379 is –5.26 msg. If we use all three galaxies - M31, M81 and NGC 3379- we obtain --5.05 msg. We will discuss the implications of these zero points later in this section. We now continue with another secondary distance indicator, the planetary nebula luminosity function.

Planetary Nebula Luminosity Function : The [OIII]λ5007 luminosity function of faint planetary nebulae follows an exponential law, but at the bright end, the function apparently shows a sharp turnover. The absolute magnitude of this truncation point has been shown to be insensitive to the age and metallicity of the parent stellar population (Jacoby, Ciardullo & Ford 1990). Thus, the PNLF method is technically applicable to all morphological types of galaxies. There are in fact several galaxies for which both Cepheid and PNLF distances are available. Among the best calibrators (LMC, M81, M31, M101), the agreement between the two distances is excellent with a very small dispersion (~2%) (Jacoby 1996). As an exercise, we show the PNLF calibration below, which will be compared with that of the SBF method in the next subsection.

The distance modulus determined by the PNLF method is expressed by:

$$(??2 - M)_{\rm PNLF} = (m^* - M^*) - 0.85A_B \qquad (5)$$

where m^* and M^* are observed and absolute turnoff magnitude respectively. Again, we adopt the M31 distance of 770 kpc. Ciardullo *et al.* (1989) obtained $m^* = 20.17$ mag for the M31 bulge. Substituting this value into equation (4), we get $M^* = -4.52$. Using only the NGC *3379* data, we obtain $M^* = -4,8]$. Calculations presented here applies only these galaxies published to date, M31, M81 and NGC 3379.

We now discuss the implications of these newly derived zero points of PNLF and SBF

methods.

Comparison of SBF and PNLF Distances : CJT reviewed the results of the two methods and analyzed the external and internal errors. They found that the PNLF distances were systematically larger than the SBF distances by 0.13 ± 0.05 mag, but concluded that this offset was fully consistent with the uncertainties in the calibration.

We have rc-calculated the SBF and PNLF distance moduli for eleven galaxies in the Leo I group, Virgo and Fornax clusters and four non-cluster galaxies, which were taken from 'l'able 3 of CJT. First, we calculated the two distance moduli using the mean zero point of three calibrators, M31, M81 and NGC 3379, Then the distances were determined by using one calibrator at a time. Using the M31 bulge only, we get a mean difference of --0.] 73:0,05 mag, which is consistent with the value determined by CJT. However, we find that if wc usc NGC 3379 as a sole calibrator, the mean difference is reduced to +-0,034- 0.05 mag. If wc usc three calibrators (M31, M81 and NGC 3379), the mean difference becomes + 0.08 ± 0.05 mag. The addition of NGC 3379 as a calibrator indeed shifts the zero point in the direction of better consistency between the two methods. Furthermore, it is encouraging that the application of NGC 3379 as a sole calibrator leads to the most consistent result between two methods, perhaps because, of three calibrators, this galaxy is the only giant elliptical galaxy, the same morphological type as target galaxies for which these distance indicators arc applied.

D_n - σ Relation : This distance estimator, developed by Dressler *et al.* (1987), correlates the velocity dispersion of elliptical galaxies with a photometric parameter D_n, which is the diameter at which the integrated surface brightness attains some defined value. The basic idea is that for a given galaxy, D_n is inversely proportional to the distance. This works because the surface brightness is independent of distance, (after correcting for K-dimming and cosmological effects). In large surveys of elliptical galaxies, the D_n - σ

relation was primarily used to measure the relative distances between clusters of galaxies, thus the lack of its zero point calibration was not so critical. There have been, however, several attempts at calibrating this relation, including Dressler (1987) where he used bulges of the spiral galaxies M31 and M81. Although the correlation may apply to spiral bulges, we must recall that the bulges have large rotational velocities in addition to the random motions measured by σ. Thus the extension of D_n -- σ to these objects assumes that all spiral bulges of a given luminosity have the same ratio of rotational velocity to velocit y dispersion. Pierce (1989) later calibrated the L — a -- Σ relation using two galaxies, NGC 3377 and NGC 3379, in the Leo I group as calibrators, assuming the distance of 10.0 ±1.0 Mpc obtained from the PNLF method (Ciardullo, Jacoby & Ford 1989) calibrated by Cepheids in M31 (Freedman & Madore 1990). However, as we know, the PNLF method itself has an uncertain zero point calibration due to the small number of calibrators. We therefore recalibrate the D_n -- σ relation using the new TRGB distance to NGC 3379.

The D_n – u relation is written as:

$$\log R_c = 1.20 \log \sigma - \log D_n - 1 \log(1 + \frac{7}{4} z) + C \qquad (G)$$

where R is the distance to the target galaxy, and a is its velocity dispersion. The third term on the right- hand side represents the cosmological correction (Lynden-Bell *et al.* 1988). The $D_n - \sigma$ distance R_c is related to the true distance R via a Malmquist correction relation:

$$R = R_c \exp[3.5(0.21)^2/N] \qquad (7)$$

where 0,21 is the dispersion in the D_n - σ relation (in units of in D_n) and N is the number of galaxies in a group. For the Leo I group, there arc two galaxies with D_n -- σ measurements, NGC 3377 and NGC 3379. Substituting $\log D_n$ = 1.24 and log a = '2.303 for NGC 3379 (Faber *et al,* 1989), wc obtain the zero point of C = 5.50. This result will be applied below to estimate the value of Hubble constant.

7.3. Determining H_0 at the Distance of the Coma Cluster

One approach which circumvents uncertainties in the Virgo velocity due to peculiar motions, is to determine H_0 at the distance of the Coma cluster, using the knowledge of the *relative* distances between Leo, Virgo and Coma. These distance ratios are well determined from various secondary- distance indicators such as the SBF, PNLF and $D_n - \sigma$ (*c.f.*, de Vaucouleurs 1 993). The Coma cluster is also attractive because its peculiar velocity is negligible compared to the redshift. Han & Mould (1992) report that the Coma redshift with respect to the cosmic microwave background is 7186 km s^{-1} while its peculiar velocity is only 4-804-428 km s^{-1}.

Recently, however, it was reported that the Coma cluster is likely to consist of two components: the central cluster centered on NGC 4874 at $cz = +6,853$ km s-1 and another centered on NGC 4839 at $cz = +7,339$ km s^{-1} (Colless & Dunn J 995). This suggests that distances to Coma obtained by various methods could be affected by a systematic error', if those samples included a substantial number of galaxies in the subcluster region around NGC 4839. We re analyzed the D_n --σ data of Faber *et al.* (1 989: F89) in order to inspect if the subclustering affects the measurement of Coma distance significantly. The Coma data in F89 is comprised of 33 elliptical galaxies, 27 of which are located within the main cluster defined by Colless & I) unn. The mean distance modulus of all 33 galaxies is 34.88 mag, while that of central 27 galaxies is 34.91 mag. Furthermore, it is noted that 3 galaxies in the main cluster have D_n -- σ distances larger than +12,000 km s^{-1}. If these galaxies are excluded from the sample, then the remaining 24 galaxies give the mean velocity of +7,195 km S^{-1}. Although the three supposedly 'background' galaxies have significantly large distances, compared to the mean, given that their redshifts do coincide with that of the Coma cluster, they are probably dynamically associated with the main cluster. We thus adopt the main Coma cluster redshift of $+6,853 \pm 100$ km s^{-1}.

The difference in distance moduli between Coma and Virgo is $\mu(\mathrm{Coma})-\mu(\mathrm{Virgo}) = 3.71 \pm 0.10$ mag (de Vaucouleurs 1993). The difference in those between Leo I and Coma is estimated by examining $D_n - \sigma$ data in F89. Applying equation (5), we obtain $\mu(\mathrm{Coma}) - \mu(\mathrm{LeoI}) = 4.7340.13$ mag. This puts the Coma cluster at $\mu = 35.024\text{-}0.37$ mag. The Hubble constant is thus 684:13 km $\mathrm{s}^{-1}\,\mathrm{Mpc}^{-1}$. We note that Tanvir *et al.* (1995) obtained $H_0 = 69 \pm 8$ km S $^{1}\mathrm{Mpc}^{-1}$ using the Cepheid observations of NGC 3368 in the Leo I group. We expect that our estimate of H_0 agrees very well with that of the Cepheid observations as we obtain the same distance to the Leo I group.

8. Uncertainties

In 'l'able 1, wc list both the random and systematic errors in the determination of the TRGB distance to NGC 3379 and the determination of H_0 based on it. One of the largest systematic uncertainty likely arises from uncertainties in the TRGB calibration at the high end of the metallicity range. We conservatively adopt an uncertainty of 0.1 mag, pending an empirical calibration of this effect. Although the Galactic globular cluster calibration covers the metallicity range only up to [Fe/H] = --0.7 dex, we note that there is a good theoretical and perhaps empirical reason to believe that the TRGB magnitude should be very close to - 4.0 mag even for higher metallicities. A linear fit to the loci of TRGB isochrone endpoints (see Figure 2 of Bica, Barbuy & Ortolani 1991) purely as a function of $(V - I)$ color suggests a slope of only $\delta I/\delta(V - I) = -10.03$ mag/mag, defined for [ire/ll] in the range between --1.7 and --0.3 dex. Also, this is confirmed by two of the highest metallicity Galactic- bulge globular clusters NGC 6553 and NGC 6528, studied in I - $(V$ -- $I)$ by Ortolani, Bica & Barbuy (1990, 1992). A fit to the upper envelope of RGB stars shows that the TRGB turns on at $M_I \simeq$ - 3.8 mag in these super- metal- rich clusters. In addition, there is good evidence for a gradient in metallicity in elliptic.als (Davies *et al.* 1993, Davidge

& Clark 1994, Thomsen & Baum 1989) and in surface brightness fluctuations in NGC 3379 (Sodeman & Thomsen 1995). Sodeman & Thomsen find the color of $(B-1) = 2.02$ at the radius of only $\sim$ 48.5 arcsec, which corresponds to the metallicity of [Fe/H] = –0,3 dex using the formula in Couture *et al.* (1 990). As indicated in Section 4, we do have good evidence from various studies that the halo of NGC 3379 is blue enough for the application of the Lee *et al.* TRGB calibration. Thus we feel that the uncertainty of 0.1 mag in the distance modulus is appropriate for this application. If, however, the metallicity of the NGC 3379 halo indeed turns out to be much higher than the value adopted in this paper (for e.g. [Fe/11] $\sim$0.0), the result would be to make the TRGB fainter. Consequently, the distance to NGC 3379 would decrease, and the value of H_0 in turn would be larger.

A major source of systematic uncertainty in the TRGB calibration comes from uncertainties in the RR Lyrae distance! scale for globular clusters, and the metallicity-magnitude relation. The absolute calibration of the TRGB method is based on the calibration of RR Lyraes in Galactic globular clusters. Lee, Freedman & Madore (I 993) adopted a calibration based on Lee, Demarque & Zinn (1990), where $M_V(RR) = 0.17[\mathrm{Fe/11}] + 0.82$, assuming $Y_{ms} = 0.23$. We note that the zero point of this adopted calibration is brighter than that of Carney, Storm & Jones (1 992), where $M_V(RR) = 0.15[1'\mathrm{c/11}] + 1.00$. Our adopted zero- point calibration is in better agreement with that of Bolte (1 995) based on a new calibration of the subdwarf main sequence, and with that of Walker (1992) based on the calibration of LMC Cepheids. The zero points in both of these cases are c.loser to $M_V \simeq 0.7$ mag. We note that if the Carney *et al.* (the intrinsically fainter calibration) had been applied to these data, the distance to NGC 3379 would be smaller ($(m - M) = 30.29$ mag), thereby raising the value of H_0 at Coma cluster to 74 ± 14 km S--1 Mpc^{-1}.

Finally, we note that when applying the TRGB method, we are comparing the halo population of NGC 3379 with that of Galactic globular clusters, which in general have

integrated colors that are different from those of elliptical halos. And the color differences often are interpreted as a difference in mean metallicity. We are not observing the red giants of globular clusters in NGC 3379. However, our adopted calibration is based on globular clusters with a range of metallicites. Then the application of the TRGB method to the halo should be valid, as long as the metallicity of the halo is not significantly outside of the calibration range.

9. summary

This paper reports the detection of red giants in a giant elliptical galaxy and explors how it can be used for the calibration of the secondary distance indicators. Individual stars identified as the Population 11 red giant branch have been detected in NGC 3379. Equating the abrupt discontinuity of the apparent luminosity function at $I = 26.29 \pm 0.14$ mag with the TRGB at $M_I = -4.0$ mag gives a distance of 11.4 ± 1.4 Mpc to NGC 3379. Extrapolating the Leo I distance to Coma using a well- determined distance ratio of two groups from $D_n - \sigma$ studies, wc measure H_0 at the distance of Coma to be 68 ± 11 km s^{-1} M])c^{-1}. Leo is the most distant application of the TRGB method to date, and is fully consistent with the Cepheid–based distance to this group as also recently determined by HST. In Figure 5, the comparison of distances derived by Cepheid 1'1, relation and TRGB method is shown, further demonstrating the accuracy of the TRGB method as a distant.c indicator.

We must not, however, be overly optimistic. At very high metallicities the calibration of the TRGB is not yet w c]] established; but an effort to obtain a more precise calibration is currently being undertaken by us. Color information on the NGC 3379 population]] would be extremely valuable in this regard. Also, even though wc are fortunate in the case of NGC 3379 to have encountered a relatively small population of intermediate- age AGB

stars, this could pose a problem in some galaxies when measuring the TRGB position using the I-band luminosity function, Nonetheless this paper gives another solid example of how powerful and promising the TRGB method can be as a distance indicator and demonstrates its versatile applicability to various types of galaxies.

We thank Dr. Peter Stetson for providing us with WFPC2 vignetting masks. This paper made use of the NASA/IPAC Extragalactic Database (NED) which is operated by the Jet Propulsion Laboratory, California Institute of Technology, under contract with the National Aeronautics and Space Administration]). BFM was supported in part by NED and by JPL. WLF was supported in part by NSF grant AST 91--16496.

REFERENCES

Bica, E., Barbuy, B. & Ortolani, S., 1991, ApJ, 382, L15

Burstein, D. & Heiles, C., 1984, ApJS, 54, 33

Capaccioli, M., Held, E. V., Lorenz, H. & Vietri, M., 1990, AJ, 99, 1813

Ciardullo, R., Jacoby, G. H. & Ford, H. C., 1989, ApJ, 344, 715

Ciardullo, R., Jacoby, G. H. & Tonry, J. J.,, 1993, ApJ, 419, 479

Colles, M. & Dunn, A. M., 1996, ApJ, 458, 435

Couture, J., Harris, W, E. & Allright, J. W. B., 1990, ApJ, 73, 671

Da Costa, G. S. & Armandroff, T. E., 1990, AJ, 100, 162

Davidge, 'T'. J. & Clark, C. C., 1994, AJ, 107, 946

Davies, R. I,., Sadler, E. & Peletier, R. F., 1993, MNRAS, 262, 650

de Vaucouleurs, G., 1975, "Stars and Stellar System" Vol. 9, University of Chicago Press, ed. A. Sandage, M. Sandage & J. Kristian .

dc Vaucouleurs, G., 1993, ApJ, 415, 10

de Vaucouleurs, C. & Capaccioli, 1979, ApJS, 40, 699

Dressler, A., Lynden-Bell, D., Burstein, D., Davies, R. I,., Faber, S. M., Terlevich, R. J. & Wegner, G., 1987, ApJ, 313, 42

Faber, S. M., Wegner, C., Burstein, D., Davies, R. 1,., Dressler, A., Lynden-Bell, D. & Terlevich, R. J., 1989, 69, 763

Ferrarese *et al., 1996,* in press

Freedman, W. I,., 1989, AJ, 98, 1285

Freedman, W. 1,. & Madore, B. F., 1990, ApJ, 365, 186

Freedman, W. I,. & Madore, B. F., 1996, ASI' Review Series, ed. V. Trimble, "Clusters, Lensing and the Future of the Universe",

Goudfrooij, P., Hansen, 1,., Jorgensen, H. E., Norgaa,rd-Nielsen, H. U., de Jong, T. & van den Hock, I,. B., 1994, A&AS, 104, 179

Graham, J. A. et al., 1996, in preparation

Green, E. M., Demarque, P. & King, C. R., 1987, The Revised Yale Isochrones and Luminosity Functions (New Haven: Yale Univ. Obs

Han, M. & Mould, J., 1990, ApJ, 360, 448

Holtzman, J. A., Burrows, C. J., Casertano, S., Hester, J. J., Trauger, J. T., Watson, A. M & Worthy, G. S., 1996, PASP, 107, 1065

Hutterer, Sasselov & Schechter 1995, AJ, 110, 2705

Iben, 1. Jr. (1988). A. S. I'. Conf. series, 1, *Progress and Opportunities in Southern Hemisphere Optical Astronomy*, eds., V. M. Blanco and M. M. Phillips, p. 220.

Iben, I. & Renzini, A. 1983, ARA&A, 21, 271

Jacoby, G. 11. 1996, private communications

Jacoby, G. 11., Ciardullo, R. & Ford, H. C., 1990, ApJ, 356, 332

Lee, S. W., 1977, A&AS, 27, 381

Lee, M. G., Freedman, W. I,. & Madore, B. F., 1993, ApJ, 417, 553

Madorc, B. F. & Freedman, W. 1,., 1995, AJ, 109, 1645

Madore, B. F., Freedman, W. I,. & Lee, M. G., 1993, AJ, 104, 2243

Mould, J. R. & Da Costa, G. W., 1988, A. S.}'. Conf. Series, 1, *Progress and (opportunities in Southern Hemisphere Optical Astronomy*, eds., V. M. Blanco and M. M. Phillips, p. 197

Mould, J. & Kristian, J., 1986, ApJ, 305, 591

Mould, J. R., Kristian, J. & Da Costa, G. S., 1983, ApJ, 270, 471

Ortiz, P., 1990, PhD Thesis, University of Toronto

Ortolani, S., Barbuy, B. & Bica, It., 1990, A&A, 236, 362

Ortolani, S., Bica, E. & Barbuy, 11., 1992, A&AS, 92, 441

Pahre, M. A. & Mould, J. R., 1994, ApJ, 433, 567

Pierce, M. J., 1989, ApJ, 344, 1,57

Sakai, S., Madore, B. F. & Freedman, W. I,., 1995, ApJ, in press

Sodeman, M. & Thomsen, B., 1994, A&A, 292, 425

Sodeman, M. & Thomsen, B., 1995, AJ, 110, 179

Stetson, P. 11., 1987, PASP, 99, 191

Stetson> P. D., 1994, PASP, 106, 250

Stetson, P. 11., 1995, Private Communication

Tanvir, N. R., Shanks, T., Ferguson, H. C. & Robinson, D. R. T., 1995, Nature, 377, 27

Thomsen, B. & Baum, W. A., 1989, ApJ, 347, 214

Tonry, J. I,., 1993, private communication, quoted by Pahre & Mould 1994

Tonry, J. J,., Ajhar, E. A. & Luppino, G. A., IWO, AJ, 100, 1416

This manuscript was prepared with the AAS LaTeX macros v3.0.

Figure Captions

Figure 1: POSS- **1** print of the area observed by HST.

Figure *2:* Reproduction of a KPNO 4m CCD frame covering a region ** X ** arcmin in the Leo I Group. The WFPC-2 footprint is shown, centered 6 arcmin east of the giant elliptical galaxy NGC 3379.

Figure *3:* *I* –band luminosity function histograms of stars found in the halo of NGC 3379.

Figure *4:* Kernel-smoothed luminosity functions (top) and their corresponding edge detection response functions (bet tom). The Sobel response function applied to the logarithmic luminosity function was weighted by suare root of the number of stars involved in the calculation.

Figure 5: TRGB edge detection response histogram from 500 iterations (see text for details). All 'signals' for *I* brighter than 26.0 mag arc very likely noise, making the TRGB detection more prominent.

Figure 6: Schematics showing the geometry of Local Group, Leo I Group and Virgo cluster used in our simple Virgocentric infall model of the velocity components (right panel).

Figure *7:* Comparison of distances obtained by the TRGB method and Cepheid PL relation. The solid line is not a fit to the data but rather a unit slope, zero- offset line.

Table 1

Error Budget

Source	Error (mag)
Random Errors:	
Galactic extinction	± 0.02
Tip Measurement	± 0.05
Leo–Coma Distance Ratio ($D_n - \sigma$)	± 0.13
Velocity of Coma (± 100 km s^{-1})	± 0.02
Total Random Uncertainty	± 0.14
Systematic Errors:	
RR Lyrae Distance Scale Zero Point	4-0.20
TRGB Metallicity Calibration	± 0.10
Photometric zero point (WFPC '2)	± 0.04
Total Systematic Uncertainty	± 0.23

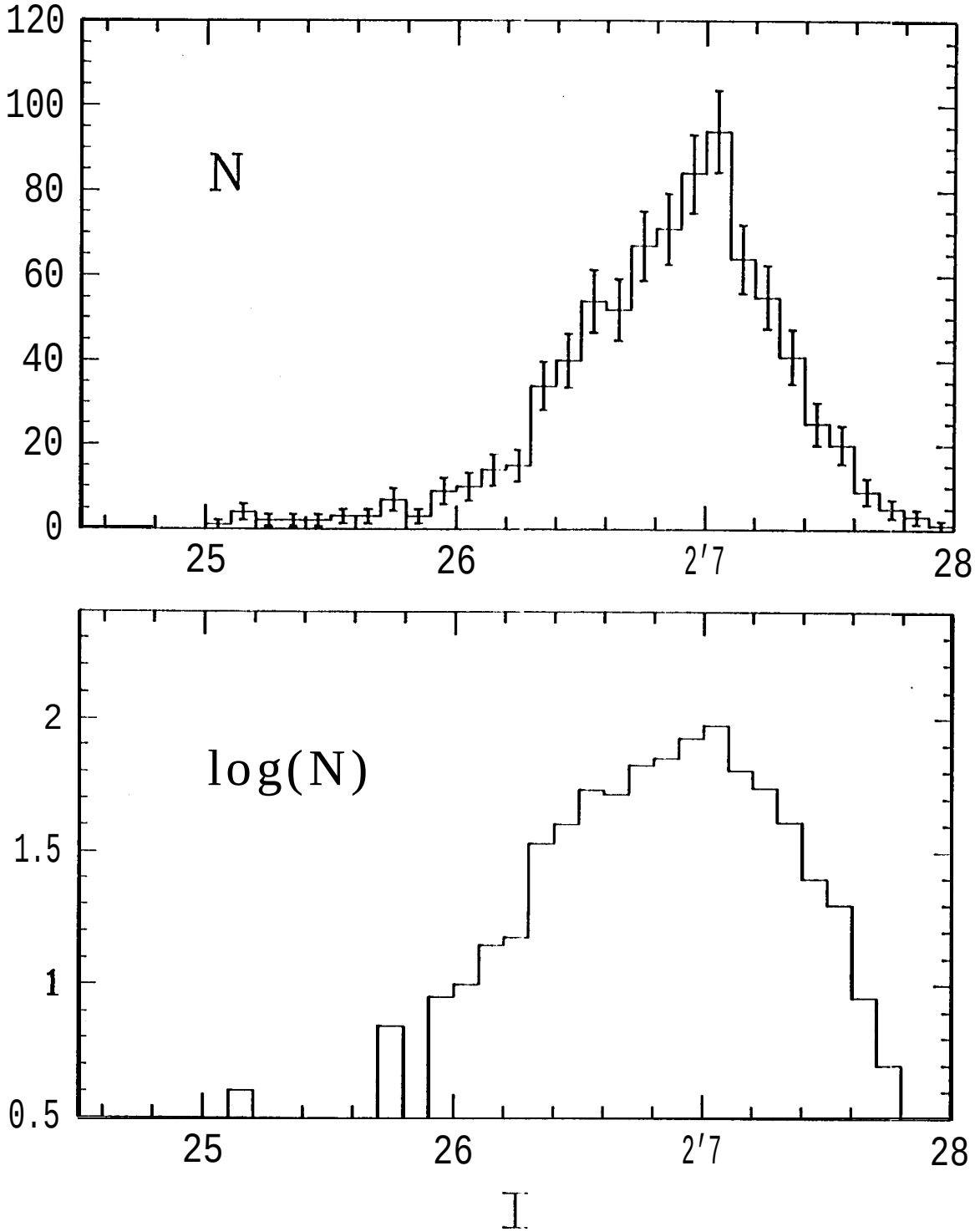
120
100
80
60
40
20
0
N
25
26
27
28
2
1.5
1
0.5
log(N)
25
26
27
28

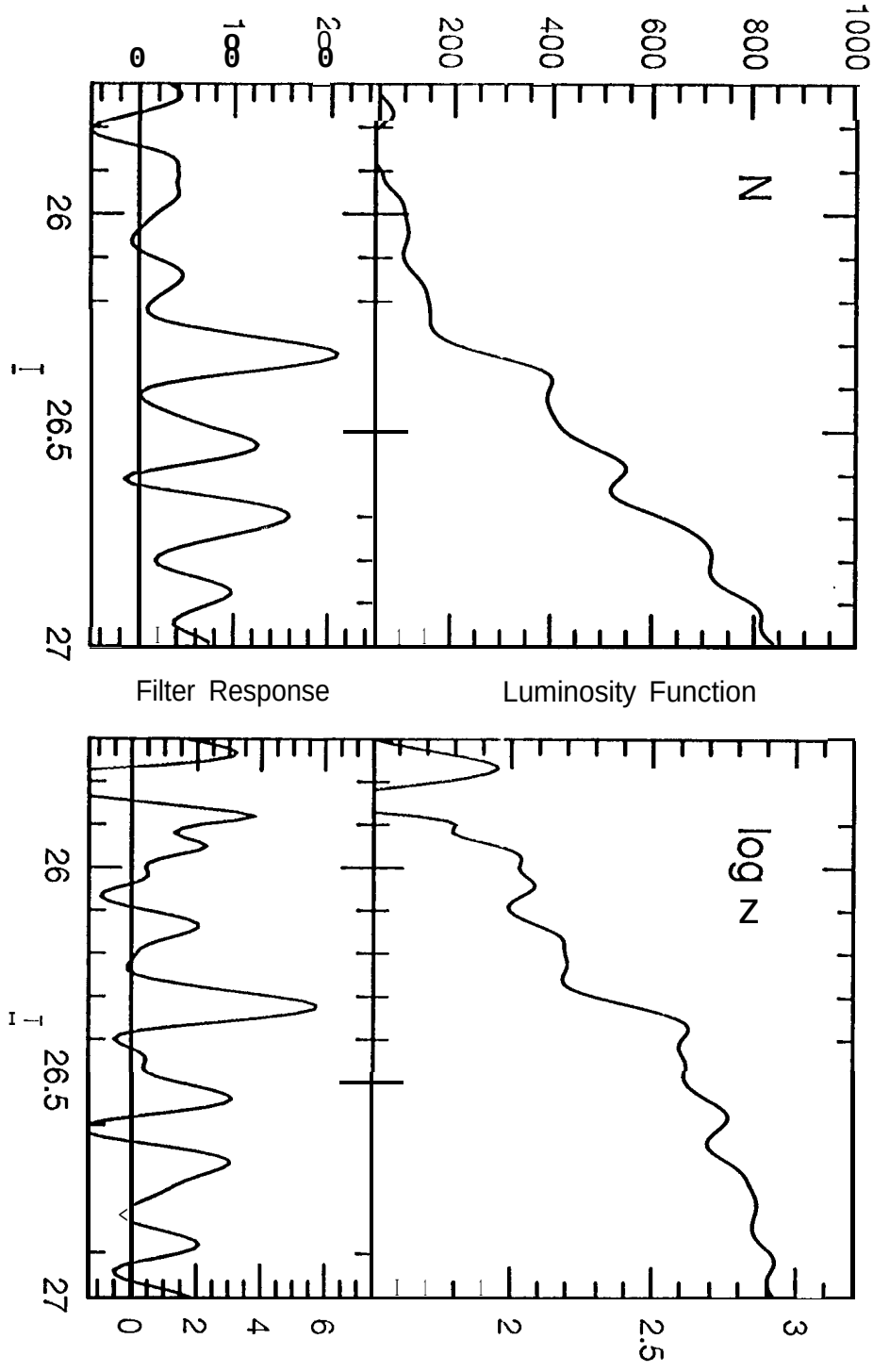
0
100
200
200
400
600
800
1000
N
26
26.5
27
I
Filter Response
Luminosity Function
log N
0
2
4
6
2
2.5
3

Response Function

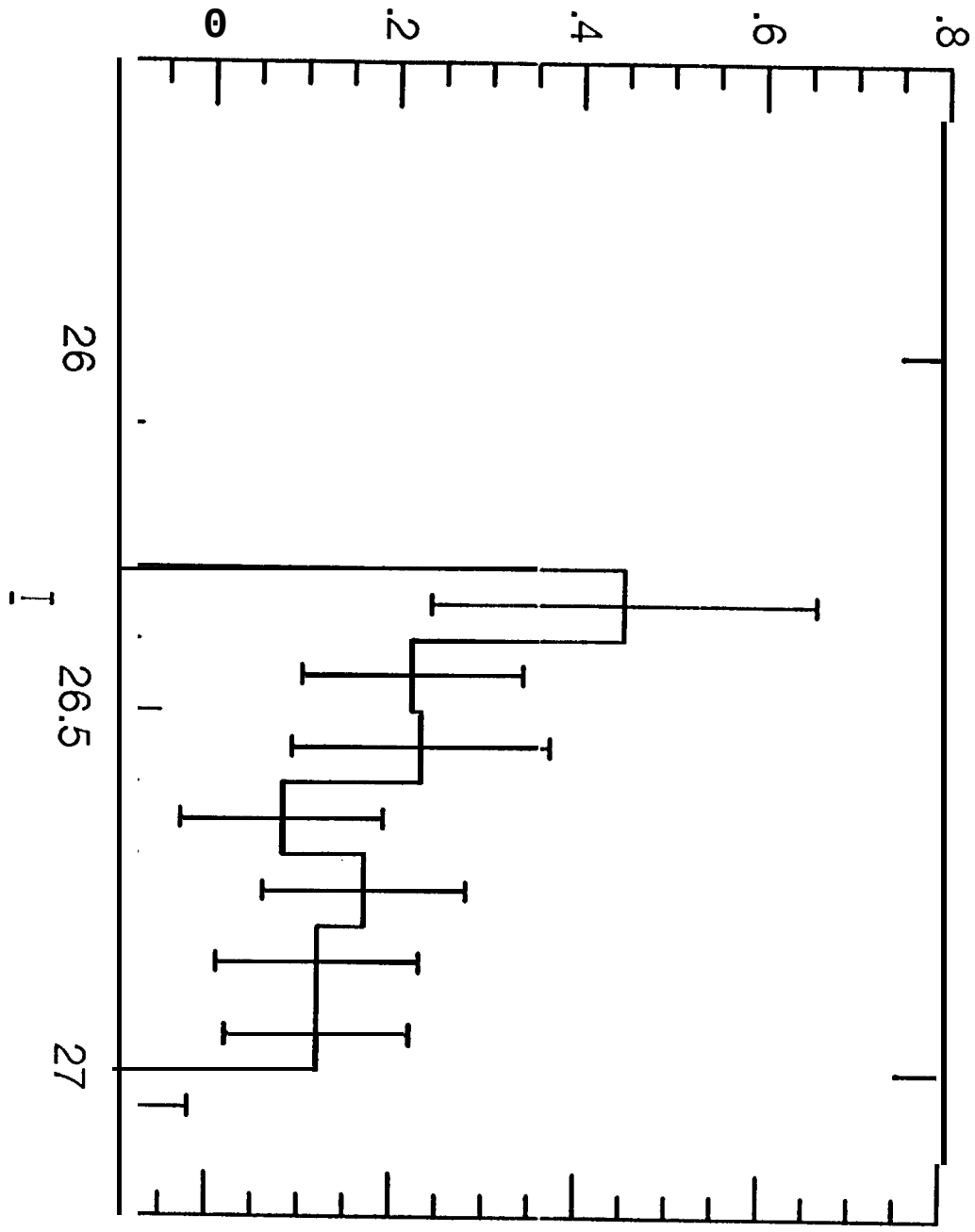

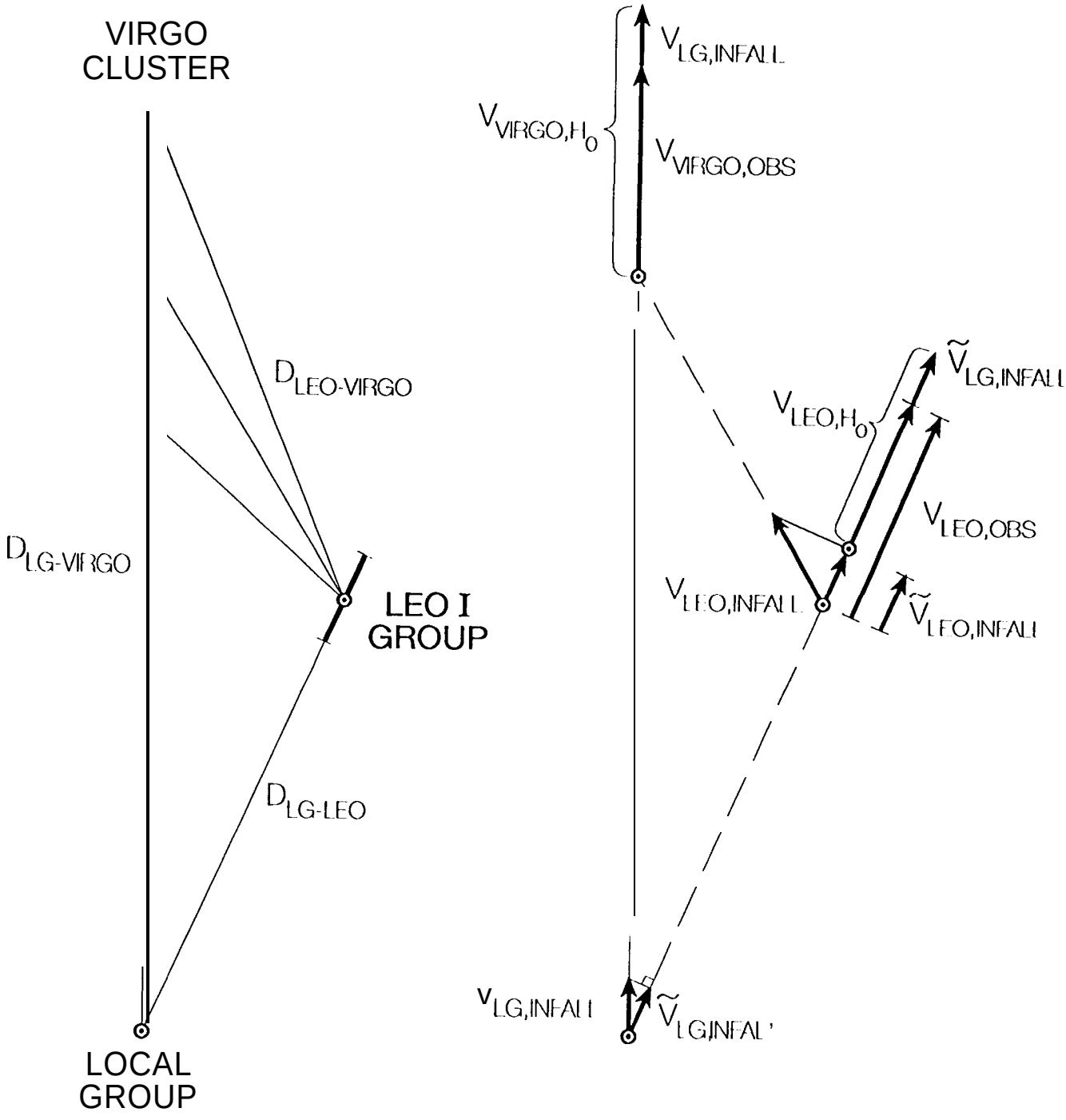
VIRGO
CLUSTER
$D_{LEO-VIRGO}$
$D_{LG-VIRGO}$
LEO I
GROUP
D_{LG-LEO}
LOCAL
GROUP
$V_{LG,INFALL}$
V_{VIRGO,H_0}
$V_{VIRGO,OBS}$
$\tilde{V}_{LG,INFALL}$
V_{LEO,H_0}
$V_{LEO,OBS}$
$V_{LEO,INFALL}$
$\tilde{V}_{LEO,INFALL}$
$V_{LG,INFALL}$
$\tilde{V}_{LG,INFALL}$

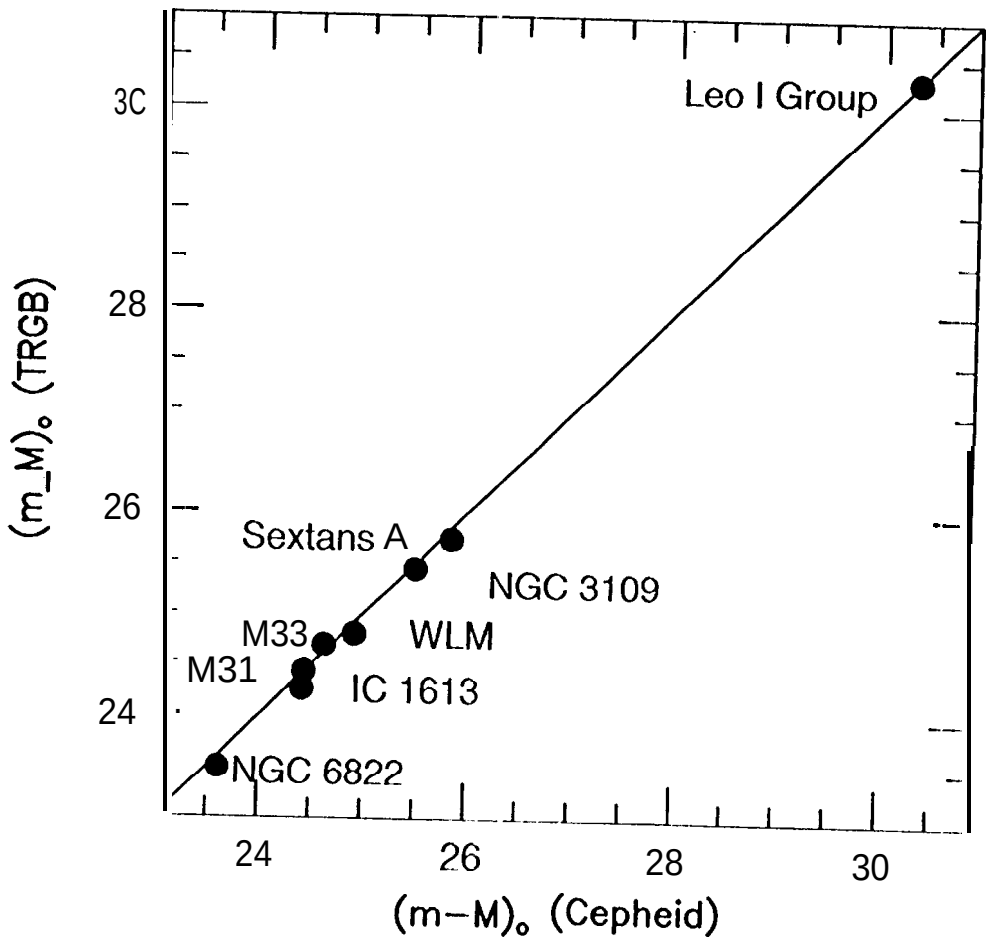
30
28
26
24
(m_M)₀ (TRGB)
Leo I Group
Sextans A
NGC 3109
M33
WLM
M31
IC 1613
NGC 6822
24
26
28
30
(m−M)₀ (Cepheid)